Copyright © 2011 Tech Science Press CMC, vol.24, no.2, pp.163-181, 2011

Vibration and Buckling of Truss Core Sandwich Plates on An Elastic Foundation Subjected to Biaxial In-plane Loads

J.W. Chen[1], W. Liu[1] and X.Y. Su[1,2]

Abstract: Truss-core sandwich plates are thin-walled structures comprising a truss core and two thin flat sheets. Since no direct analytical solution for the dynamic response of such structures exists, the complex three dimensional (3D) systems are idealized as equivalent 2D homogeneous continuous plates. The macroscopic effective bending and transverse shear stiffness are derived. Two representative core topologies are considered: pyramidal truss core and tetrahedral truss core. The first order shear deformation theory is used to study the flexural vibration of a simply supported sandwich plate. The buckling of the truss core plate on an elastic foundation subjected to biaxial in-plane compressive loads is also investigated. It's found that the lowest buckling loads and modes are dependent on the foundation stiffness as well as bending and transverse shear stiffness of the plate. The geometric parameters of a sandwich plate are optimized to obtain strongest buckling resistance per unit weight. To verify the accuracy of analytical solutions, 3D finite element (FE) models are established, and good agreement is observed between them. It's obvious that the homogenization procedure leads to great savings in computational effort.

Keywords: Vibration, Buckling, Truss core, Plate, Minimum-weight optimization.

1 Introduction

Sandwich structures, comprising two thin stiff face-sheets and a thick low-density core, have been used widely for aerospace, marine and civil engineering applications (Vinson, 1999). The face-sheets can be different in material and thickness, which primarily resist in-plane loads and bending loads. The core can be foam, solid, honeycomb, corrugated or truss core, which primarily resists transverse shear loads. There is plenty of work to discuss the mechanical properties (Johnson and

[1] Peking Univ, LTCS and Dept Mech & Aero Engn, Coll Engn, Beijing 100871, China.
[2] Corresponding author, Email address: xyswsk@pku.edu.cn (X.Y. Su).

Sims, 1986), elastic stability (Pahr and Rammerstorfer, 2006), dynamic response (Qiu, Deshpande and Fleck, 2003) and structural optimization (Tapp, Hansel and Mittelstedt et al., 2004; Khoshravan and Hosseinzadeh, 2009) of sandwich structures. Recently truss core sandwich structures receive much attention from researchers because they promise higher stiffness to weight and strength to weight ratios than those of foam or honeycomb cores. In addition, the truss cores have open channels for multifunctional application such as active cooling (Lu, Valdevit and Evans, 2005).

The truss cores are constituted of periodically distributed struts, with topologies such as pyramid and tetrahedron. A lot of literature is concerning these core topologies. Wicks and Hutchinson (2001) published a study on the optimal design of sandwich plates comprising a tetrahedral truss core and either solid or triangulated face-sheets. They found the weights of the optimized truss core plates for a given bending and shear load were similar with honeycomb-core sandwiches. Wallach and Gibson (2001) investigated the stiffness and strength of a 3D truss structure comprising two triangulated faces and a pyramidal truss core with experimental and finite element methods. Deshpande and Fleck (2001) studied the collapse response of tetrahedral truss core sandwich beams and proposed four collapse mechanisms which include face-yield, face-wrinkling, indention and core shear. The impulse-resistance (Hutchinson and Xue, 2004) and impact response (Yungwirth, Wadley and O'Connor et al., 2008) of truss core plates are also investigated.

The sandwich plates may be used to bear dynamic loads which may govern the structural design. Therefore it is necessary to learn the vibration response of these plates. However the truss core plates are such complex 3D systems that direct analytical solution does not exist. The 3D finite element (FE) method is usually employed for structural analysis and design, but huge computational efforts would be required for large complex structures, and that is uneconomic. However, the 3D system may be idealized as an equivalent homogeneous continuous plate, and then solutions based on the plate theory can be obtained. On the other hand, 2D FE analysis could be performed with the equivalent plate. The degrees of freedom can be reduced significantly. A lot of literatures discuss about the homogenization techniques. Lok and Cheng (2000) derived the equivalent stiffness of a 2D orthotropic sandwich panel and obtained good agreement of response between analytical solutions and FE results. Ziegler, Accorsi and Bennett (2004) presented a general method to model the lattice block material as a continuum plate. Bending and in-plane behavior of the continuum plate model agrees well with the FE model. Rabczuk et al. (2004) proposed a homogenization method for sandwich structures with 2D cores to study the dynamic response when subjected to impulse or blast loading. Xue, Vaziri and Hutchinson (2005) proposed a constitutive model to study the elastic-plastic behavior of compressible square honeycomb sandwich plates. Liu, Deng and Lu (2007) proposed an equivalent single layered FE computational model to predict the structural behavior of prismatic and truss-core sandwich panels.

However, little literature is found concerning the flexural vibration of the truss core plates subjected to in-plane loads, which may have a significant influence on vibration frequencies and stability. In sandwich structures for given load type and boundary conditions, an infinite number of bucking loads exist mathematically but only the lowest value has physical significance. The authors are primarily concerned about the overall instability of the sandwich plates. In service, sandwich panels may be settled on flexible supports or foundations. Then the foundation stiffness may have an effect on the buckling loads and modes. The present study is structured as follows. First, the macroscopic effective properties of the plates are derived. Second, by taking into account of the transverse shear, the governing equations of an equivalent continuum plate are derived. The expressions of natural frequencies and buckling loads are given. Third, the effects of in-plane loads and geometric parameters on natural frequencies are investigated. Fourth, the influence of elastic foundation modulus on bucking loads and modes is investigated. The commercial finite element code, ANSYS is employed to establish 3D full-size models to verify the accuracy of the solutions. In the end, the geometric parameters of the sandwich configuration are optimized to attain strongest buckling resistance by minimum weight.

2 Effective properties of truss core sandwich plate

A sandwich panel may be idealized as an equivalent plate which is homogeneous and continuous. Because the transverse shear stiffness is relatively weak, the shear deformation in the transverse direction must be taken into account. The equivalent plate may be transverse isotropic, orthotropic or anisotropic, dependent on face-sheet material properties and constitution of the truss core. In this paper, the face sheets and truss members are made of isotropic materials. To obtain the effective elastic constants, the following assumptions are made:

1. The face sheets are thin and stiff compared with the truss core. The transverse shear deformation in the face sheets is neglected.

2. The truss core is seemed as a pin-jointed assembly and makes no contribution to the overall bending stiffness.

3. Deformation of the truss members and face sheets is small; local buckling of the face sheets does not occur.

4. Straight lines normal to the middle plane remain straight in distortion, but rotate through a small angle due to transverse shear deformation.

5. A sandwich plate comprises plenty of unit cells in both length and width directions.

Fig. 1 shows the unit cells of the truss core plates with (a) pyramidal topology and (b) tetrahedral topology. The upper and lower face sheets have the same thickness t_f. The unit cell size and core height are d and h_c, respectively. All struts share the same length L_c and cross-sectional area A_c. The symmetrical configuration of both cores implies transverse isotropy of elastic constants.

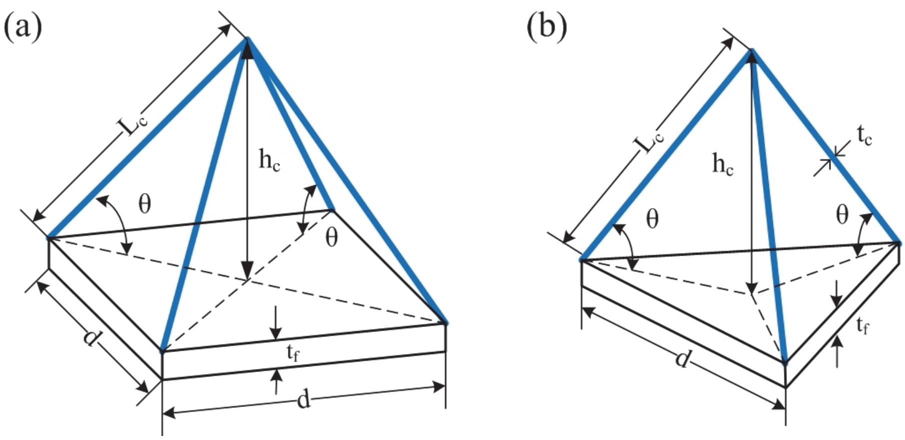

Figure 1: The unit cells of the truss core plates with (a) pyramidal topology and (b) tetrahedral topology (absent the top face sheet)

2.1 Bending stiffness

Based on the first order shear deformation theory (Mindlin, 1951), the displacement field of a continuum plate can be written as:

$$
\begin{aligned}
u &= -z\psi_x(x,y,z,t) \\
v &= -z\psi_y(x,y,z,t) \\
w &= w_0(x,y,z,t)
\end{aligned}
\tag{1}
$$

where z is the coordinate perpendicular to the mid-plane; w_0 is the lateral deflection of a point on the mid-plane; t denotes time; and ψ_x, ψ_y are rotations of the normal to the mid-plane about the y- and x-axes, respectively.

The strain-displacement relations are given as follows:

$$\begin{aligned}
\varepsilon_x &= -z\frac{\partial \psi_x}{\partial x} \\
\varepsilon_y &= -z\frac{\partial \psi_y}{\partial y} \\
\gamma_{xy} &= -z\left(\frac{\partial \psi_x}{\partial y} + \frac{\partial \psi_y}{\partial x}\right)
\end{aligned} \tag{2}$$

Stress-strain relations of the thin face sheets are:

$$\begin{Bmatrix} \sigma_x \\ \sigma_y \\ \sigma_{xy} \end{Bmatrix} = \frac{E_f}{1-\nu^2}\begin{bmatrix} 1 & \nu & 0 \\ \nu & 1 & 0 \\ 0 & 0 & \frac{1-\nu}{2} \end{bmatrix}\begin{Bmatrix} \varepsilon_x \\ \varepsilon_y \\ \varepsilon_{xy} \end{Bmatrix} \tag{3}$$

Therefore the bending stiffness arising from the face sheets is described as:

$$D_f = 2\int_{h_c/2}^{h_c/2+t_f} \frac{E_f z^2}{1-\nu^2}dz = \frac{E_f t_f h^2}{2(1-\nu^2)} + \frac{E_f t_f^3}{6(1-\nu^2)} \tag{4}$$

where $h = h_c + t_f$, is the distance between the mid-planes of upper and lower face sheets; the latter item is usually enough small to be neglected because $t_f/h_c << 1$; E_f and ν are the Young's modulus and Poisson's ratio of the face sheets, respectively.

Following the assumptions, the truss core does not contribute to the overall bending stiffness, hence the relations between the overall bending moments and displacements are given by:

$$\begin{aligned}
M_x &= -D\left(\frac{\partial \psi_x}{\partial x} + \nu\frac{\partial \psi_y}{\partial y}\right) \\
M_y &= -D\left(\frac{\partial \psi_y}{\partial y} + \nu\frac{\partial \psi_x}{\partial x}\right) \\
M_{xy} &= -\frac{1-\nu}{2}D\left(\frac{\partial \psi_x}{\partial y} + \frac{\partial \psi_y}{\partial x}\right)
\end{aligned} \tag{5}$$

where $D = D_f$, is the equivalent overall flexural rigidity.

2.2 Transverse shear stiffness

In this paper, the core struts are modeled as simple truss members, whose endpoints are pin-jointed. The length to thickness ratio of the struts is big enough to neglect the bending effect. In "stretching-dominated" truss materials, the stretching stiffness plays a major role in structural mechanical behavior (Deshpande, Ashby and Fleck, 2001). Following the assumptions, the shear rigidity of the core can be derived from the relations between the axial forces and displacements, and then the equivalent transverse shear stiffness of the sandwich plate can be obtained in terms of core shear rigidity.

$$C_{pry} = G^c_{pry} h_c = \frac{E_c A_c \sin^3\theta}{h_c} \tag{6}$$

$$C_{tet} = G^c_{tet} h_c = \frac{E_c A_c \sin^3\theta}{\sqrt{3} h_c} \tag{7}$$

where C_{pry} and C_{tet} are the transverse shear stiffness of the pyramidal and tetrahedral truss core plate, respectively; E_c is the Young's modulus of the core struts.

It should be emphasized that the equivalent elastic constants are approximate analytical expressions, due to neglect of shear deformation in face sheets and bending deformation in struts. However, when the face sheets are thin enough compared with the core height and the slenderness ratio of the struts is sufficiently large, accuracy of the analytical expressions will be guaranteed.

3 Free vibration and buckling

3.1 Governing equations

Consider a sandwich plate on Winkler foundation subjected to biaxial in-plane compressive loads, as shown in Fig. 2. On the basis of first order shear deformation theory, the differential equations of free motion are given as

$$C\left(\frac{\partial w^2}{\partial x^2} - \frac{\partial \psi_x}{\partial x}\right) + C\left(\frac{\partial w^2}{\partial y^2} - \frac{\partial \psi_y}{\partial y}\right) - P_x\frac{\partial w^2}{\partial x^2} - P_y\frac{\partial w^2}{\partial y^2} - Kw = \rho h\frac{\partial w^2}{\partial t^2} \tag{8}$$

$$C\left(\frac{\partial w}{\partial x} - \psi_x\right) + D\left(\frac{\partial \psi_x^2}{\partial x^2} + \frac{1-\nu}{2}\frac{\partial \psi_y^2}{\partial y^2} + \frac{1+\nu}{2}\frac{\partial \psi_y^2}{\partial x \partial y}\right) = J_x\frac{\partial \psi_x^2}{\partial t^2} \tag{9}$$

$$C\left(\frac{\partial w}{\partial y} - \psi_y\right) + D\left(\frac{\partial \psi_y^2}{\partial y^2} + \frac{1-\nu}{2}\frac{\partial \psi_x^2}{\partial x^2} + \frac{1+\nu}{2}\frac{\partial \psi_x^2}{\partial x \partial y}\right) = J_y\frac{\partial \psi_y^2}{\partial t^2} \tag{10}$$

Where C and D are the equivalent transverse shear stiffness and flexural rigidity; K is the foundation stiffness per unit area; ρh is the weight of the panel per unit area; P_x and P_y are the compressive loads per unit width; P_x and $P_y$can be positive or negative, so that tension is included; J_x and J_y are moments of inertia per unit

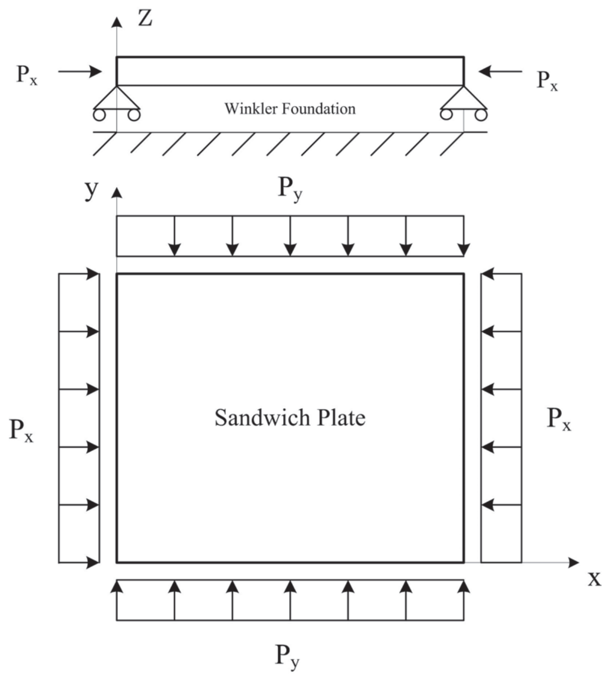

Figure 2: A plate on Winkler foundation subjected to in-plane loads

area of the cross section. As is well known, the cellular truss core panel has a very small relative density, so the rotary inertia of the panel will be neglected in future discussion.

Adding the differentiation of Eq.9 with respect to x and Eq.10 with respect to y, yields:

$$C\nabla^2 w + D\nabla^2 \psi - C\psi = 0 \tag{11}$$

where ∇^2 is Laplace's operator; and ψ is defined as:

$$\psi = \frac{\partial \psi_x}{\partial x} + \frac{\partial \psi_y}{\partial y} \tag{12}$$

Substitution of Eq.12 into Eq.8 yields:

$$C\nabla^2 w - C\psi - Kw - P_x \frac{\partial w^2}{\partial x^2} - P_y \frac{\partial w^2}{\partial y^2} - \rho h \frac{\partial w^2}{\partial t^2} = 0 \tag{13}$$

Elimination of ψ from Eq.11 and Eq.13 yields:

$$\left(1-\frac{P_x}{C}\right)\frac{\partial w^4}{\partial x^4}+\left(1-\frac{P_y}{C}\right)\frac{\partial w^4}{\partial y^4}+\left(2-\frac{P_x+P_y}{C}\right)\frac{\partial w^4}{\partial x^2\partial y^2}+\left(\frac{P_x}{D}-\frac{K}{C}\right)\frac{\partial w^2}{\partial x^2}$$
$$+\left(\frac{P_y}{D}-\frac{K}{C}\right)\frac{\partial w^2}{\partial y^2}+\frac{K}{D}w-\frac{\rho h}{C}\left(\frac{\partial w^4}{\partial x^2\partial t^2}+\frac{\partial w^4}{\partial y^2\partial t^2}\right)+\frac{\rho h}{D}\frac{\partial w^2}{\partial t^2}=0 \tag{14}$$

Eq.14 may be simplified for the free vibration of a beam as:

$$\left(1-\frac{P_x}{C}\right)\frac{\partial w^4}{\partial x^4}+\left(\frac{P_x}{D}-\frac{K}{C}\right)\frac{\partial w^2}{\partial x^2}+\frac{K}{D}w-\frac{\rho h}{C}\frac{\partial w^4}{\partial x^2\partial t^2}+\frac{\rho h}{D}\frac{\partial w^2}{\partial t^2}=0 \tag{15}$$

3.2 Natural frequencies

Consider a rectangular plate to be simply supported at all edges, the displacement boundary conditions are written as:

$$\begin{aligned} x=0,\quad a:\quad & w=\psi_y=\frac{\partial \psi_x}{\partial x}=0 \\ y=0,\quad b:\quad & w=\psi_x=\frac{\partial \psi_y}{\partial y}=0 \end{aligned} \tag{16}$$

For harmonic motion, the deflection and rotations of the plate can be expressed as:

$$w=A_{mn}\sin\left(\frac{m\pi x}{a}\right)\sin\left(\frac{n\pi y}{b}\right)\sin(\omega t+\phi) \tag{17}$$

$$\psi_x=B_{mn}\cos\left(\frac{m\pi x}{a}\right)\sin\left(\frac{n\pi y}{b}\right)\sin(\omega t+\phi) \tag{18}$$

$$\psi_y=C_{mn}\sin\left(\frac{m\pi x}{a}\right)\cos\left(\frac{n\pi y}{b}\right)\sin(\omega t+\phi) \tag{19}$$

where A_{mn}, B_{mn} and C_{mn} are unknown constants; ω and ϕ are radial frequency and initial phase angle, respectively.

Substituting Eq.17 into Eq.14, one can obtain

$$s_1-P_xs_2-P_ys_3+Ks_4=\omega_{mn}^2\rho hs_4 \tag{20}$$

where

$$
\begin{aligned}
s_1 &= \left(\left(\frac{m\pi}{a}\right)^2 + \left(\frac{n\pi}{b}\right)^2\right)^2 \\
s_2 &= \frac{1}{C}\left(\frac{m\pi}{a}\right)^2\left(\left(\frac{m\pi}{a}\right)^2 + \left(\frac{n\pi}{b}\right)^2\right) + \frac{1}{D}\left(\frac{m\pi}{a}\right)^2 \\
s_3 &= \frac{1}{C}\left(\frac{n\pi}{b}\right)^2\left(\left(\frac{m\pi}{a}\right)^2 + \left(\frac{n\pi}{b}\right)^2\right) + \frac{1}{D}\left(\frac{n\pi}{b}\right)^2 \\
s_4 &= \frac{1}{C}\left(\left(\frac{m\pi}{a}\right)^2 + \left(\frac{n\pi}{b}\right)^2\right) + \frac{1}{D}
\end{aligned}
\tag{21}
$$

Then the natural frequencies of flexural vibration are obtained as follows

$$
\omega_{mn} = \left(\frac{s_1 - P_x s_2 - P_y s_3 + K s_4}{\rho h s_4}\right)^{1/2} \tag{22}
$$

3.3 Overall buckling

The truss core sandwich plates may collapse by overall buckling, local face buckling or core strut buckling. The former buckling mode is to be discussed in the present work. Suppose that the plate is subjected to biaxial in-plane compressive loads ($P_x > 0, P_y > 0$). As is known to all, when the natural frequency of a system vanishes, the system begins to buckle. Introduce $\omega_{mn} = 0$ into Eq.20, one can obtain

$$
s_1 - P_x s_2 - P_y s_3 + K s_4 = 0 \tag{23}
$$

For simplicity, define

$$
\varphi = P_y / P_x \tag{24}
$$

Substitution of Eq.24 into Eq.23 yields:

$$
P_x^{cr} = \frac{s_1 + K s_4}{s_2 + \varphi s_3} \tag{25}
$$

which is the critical buckling load in the x-direction corresponding to vibration mode (m, n). m and n represent the number of half wavelengths in the x- and y-directions, respectively.

With Eq.25 and Eq.21, it's shown that for a given sandwich plate, the critical buckling load corresponding to mode (m, n) depends on the biaxial load ratio ϕ as well as the foundation modulus K. It is observed that the buckling load P_x^{cr} decreases as ϕ increases and increases as K grows. It should be emphasized that all values of P_x^{cr} with different pairs of (m, n) exist mathematically, but only the lowest value results in buckling. This lowest value does not always correspond to mode (1, 1), due to the effect of foundation stiffness.

4 Results and discussion

As numerical examples, the face sheets and core struts of the sandwich plates are all made of steel, with Young's modulus E = 210GPa, Poisson ratio ν = 0.3 and mass density ρ = 7800kg/m^3. Two sandwich plates are considered. Plate A: a pyramidal truss core plate with 25 unit cells in both$x-$ and $y-$ directions; plate B: a tetrahedral truss core plate with 16 cells in the x-direction and 20 cells in the y-direction. The cross section of the struts is square with the thickness of t_c. The geometric parameters of the two plates are given in Tab. 1. To verify the accuracy of analytical solutions, 3D full-size models are established using a commercial finite element code, ANSYS. The face sheets and core struts are modeled with shell element Shell99 and beam element Beam4, respectively. Shell99 is an eight-node quadrilateral shell element which has six degrees of freedom at each node. Shell99 includes the input option of elastic foundation stiffness and is characterized by the ability to offset the nodes from mid-plane to top or bottom face. Beam4 is a uniaxial element with the capabilities of bending, torsion, tension and compression, which also has six degrees of freedom at each node. Hence the nodes of beam and shell elements can be coupled perfectly. Fig. 3 shows the 3D FE model of one quarter of Plate B.

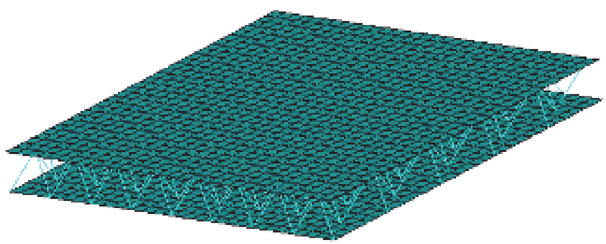

Figure 3: 3D FE model of one quarter of plate B

4.1 Natural frequency analysis

Without consideration of in-plane loads and elastic foundation, the natural frequencies of the sandwich plates are calculated first. In order to investigate the influence of transverse shear, let C$\rightarrow\infty$, as well as P_x= P_y= K= 0 in Eq.22, we obtain the solutions based on the Thin Plate Theory (TPT) which doesn't take into account of transverse shear. Tab. 2 shows the first eight natural frequencies of the two plates with all edges simply supported. For plate A, the vibration mode (m,n) and (n,m)

have the same value of frequency due to structural symmetry. To validate the analytical solutions, FE results are calculated by ANSYS via mode analysis. It's shown that when transverse shear deformation is not included, large errors generate even the sandwich plate is very thin (a/h>30 for plate A). This is due to the weak shear stiffness of the truss core. The analytical solutions including the effect of transverse shear are in very good agreement with 3D FE results. For both of the computational models, the largest error is less than 3%, occurring in the eighth mode.

For the convenience of discussion, only plate A is considered in the following part. Fig. 4 shows the influence of face-sheet thickness and core strut thickness on the fundamental natural frequency. The length and width of the plate are fixed as the same in Tab. 2. The core height is also kept constant. It can be seen from the figure that for a given value of t_f, frequency climbs up to a peak value and then decline. The peak values increase as t_f increases. Fig. 5 shows the influence of unit cell size on the fundamental frequency. It can be seen that for a given value of t_c, frequency increase to a peak value as d grows, and then falls. It's also shown that as t_c grows, the peak value first increase and then decline.

Table 1: The geometric parameters of the two sandwich plates

Plate	t_f(m)	h_c(m)	t_c (m)	d(m)	a(m)	b(m)
A	0.0025	0.0300	0.003	0.0424	1.06	1.06
B	0.0035	0.0612	0.004	0.0750	1.20	1.30

Table 2: The first eight natural frequencies of the two plates

<table>
<tr><th colspan="2">Mode</th><th colspan="3">Plate A (Pyramidal)</th><th colspan="3">Plate B (Tetrahedral)</th></tr>
<tr><th>m</th><th>n</th><th>TPT</th><th>Present</th><th>3D FE</th><th>TPT</th><th>Present</th><th>3D FE</th></tr>
<tr><td>1</td><td>1</td><td>228.20</td><td>204.93</td><td>203.72</td><td>340.71</td><td>227.30</td><td>226.07</td></tr>
<tr><td>1</td><td>2</td><td rowspan="2">570.51</td><td rowspan="2">451.02</td><td rowspan="2">445.10</td><td>811.32</td><td>407.24</td><td>403.93</td></tr>
<tr><td>2</td><td>1</td><td>892.21</td><td>432.03</td><td>427.91</td></tr>
<tr><td>2</td><td>2</td><td>912.82</td><td>652.01</td><td>640.37</td><td>1362.8</td><td>556.94</td><td>549.40</td></tr>
<tr><td>1</td><td>3</td><td rowspan="2">1141.0</td><td rowspan="2">769.27</td><td rowspan="2">752.51</td><td>1595.7</td><td>610.16</td><td>600.46</td></tr>
<tr><td>3</td><td>1</td><td>1811.4</td><td>655.82</td><td>643.37</td></tr>
<tr><td>2</td><td>3</td><td rowspan="2">1483.3</td><td rowspan="2">927.07</td><td rowspan="2">903.89</td><td>2147.2</td><td>721.47</td><td>705.58</td></tr>
<tr><td>3</td><td>2</td><td>2282.0</td><td>746.26</td><td>728.66</td></tr>
</table>

Fig. 6 shows the variation of the first four natural frequencies with the applied bidirectional in-plane loads in both $x-$ and $y-$directions ($\phi = 1$). Vibration mode (m,n) and (n,m) share the same frequencies because the plate is square and the

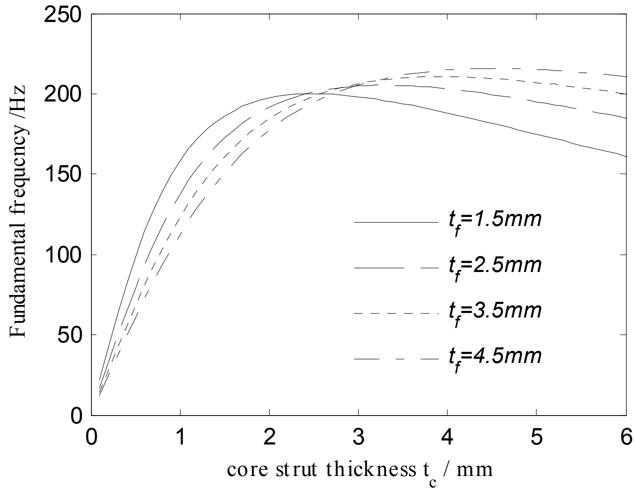

Figure 4: Fundamental frequency versus core strut thickness t_c (h_c = 0.03m, d = 0.0424m)

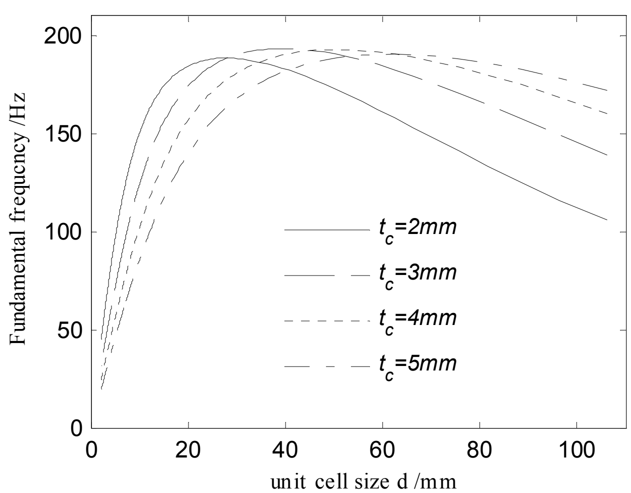

Figure 5: Fundamental frequency versus unit cell size d (h_c = 0.03m, t_f = 0.0025m)

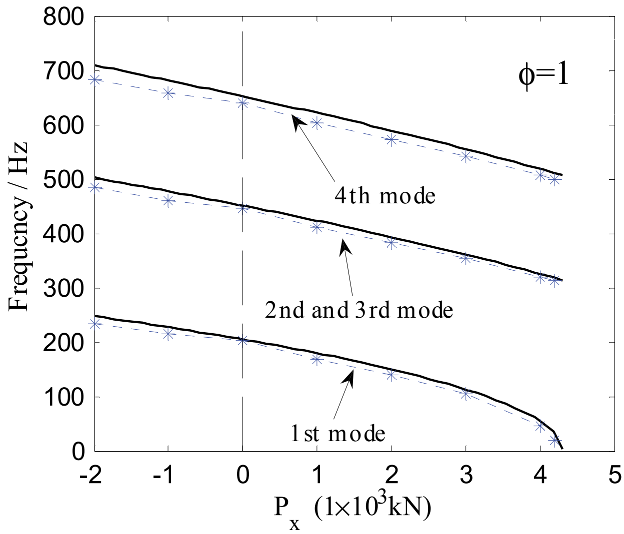

Figure 6: Variation of frequency with the applied bidirectional in-plane loads (ϕ = 1)

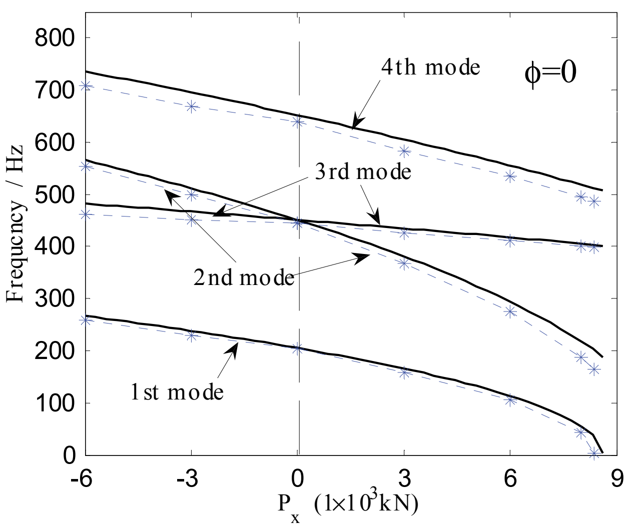

Figure 7: Variation of frequency with the applied unidirectional in-plane load (ϕ = 0)

loads in both directions are equal. Fig. 7 shows the variation of the first four natural frequencies with the unidirectional load in the x-direction (ϕ = 0). The 2^{nd} and 3^{rd} modes correspond to mode (2, 1) and (1, 2), respectively. The values indicated along the vertical dashed lines are the natural frequencies when the in-plane loads are zero. In general, compressive loads reduce the natural frequencies while tensile loads raise the natural frequencies. The points at which the curves intersect the x-axis indicate the critical buckling loads. The dot lines with markers'*' are calculated from 3D FE models. Good agreement is observed between the analytical solutions and FE results.

4.2 Buckling analysis

The overall buckling of sandwich plates was investigated in chapter 3.3. With Eq.25 the buckling loads of plate A can be calculated. To validate the present solutions, eigenbuckling analysis of the full-size model is performed using ANSYS. Fig. 8 shows the buckling loads versus biaxial load ratio ϕ for $K = 0$. The curves of the second mode and the third mode intersect at ϕ = 1, due to equal loading in both directions.Fig. 9 and Fig. 10 show the effects of foundation stiffness, where K_0= 1×10^4kN/m^3. Compared with Fig. 8, it can be seen that the foundation stiffness has a most significant influence on the first mode. In both figures the first mode is elevated so much to intersect the second mode at the point P. At the left side of point P, mode (2, 1) results in the lowest buckling load; while at the right side of point P, mode (1, 1) gives the lowest buckling load. In Fig. 10 point P moves towards ϕ = 1 as the foundation stiffness grows from $5K_0$ to $8K_0$. The position of point P depends on the combination of foundation stiffness, bending stiffness and shear stiffness of the sandwich plate. The markers'*' are the lowest buckling loads calculated from 3D FE models, corresponding to different values of ϕ. It can be seen that the lowest buckling loads given by the present solutions are in good agreement with the FE results.

4.3 Minimum-weight optimization for buckling resistance

In engineering field, sandwich structures are expected to resist the applied loads by minimum weight. Designers may search for the minimum-weight solution by examining all the possible combinations of geometric parameters and materials. However, a lot of time will be consumed due to lack of experience. For a sandwich plate with a specified core topology, if the length and width is kept constant, there remain four variables to specify. They are the face-sheet thickness t_f, core height h_c, unit cell size d, and core strut thickness t_c. In general, increase of t_f and h_c results in larger flexural rigidity, and increase of t_c results in larger transverse shear rigidity. They both improve the buckling resistance as well as increase the total

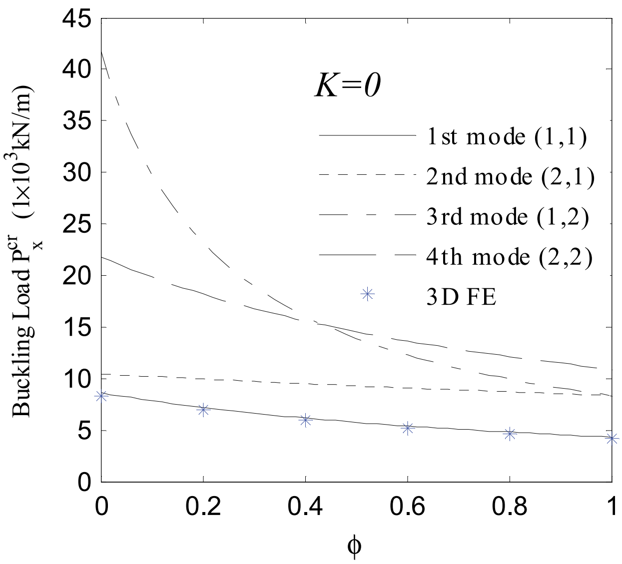

Figure 8: Buckling loads versus biaxial compressive load ratio ϕ (K = 0)

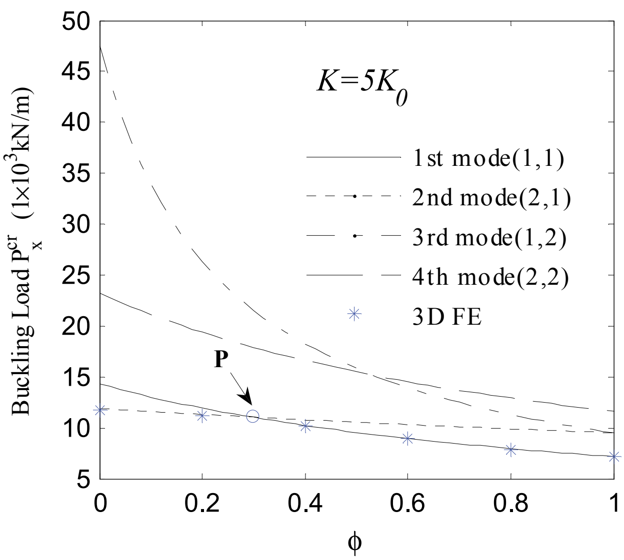

Figure 9: uckling loads versus biaxial compressive load ratio ϕ (K = $5K_0$).

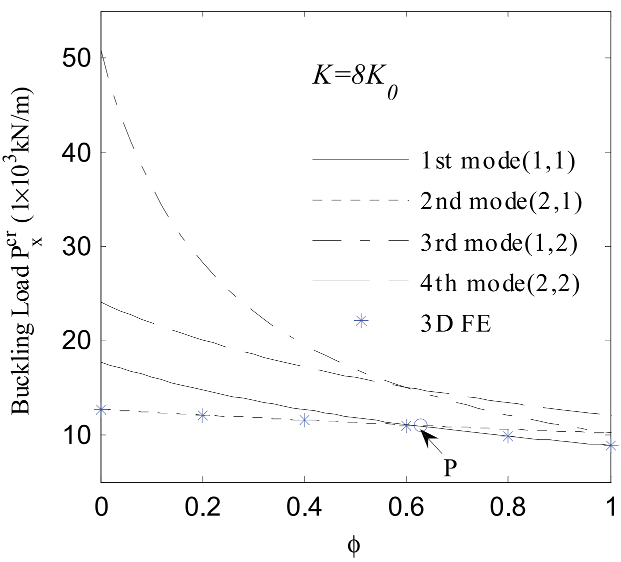

Figure 10: Buckling loads versus biaxial compressive load ratio ϕ (K = 8K_0).

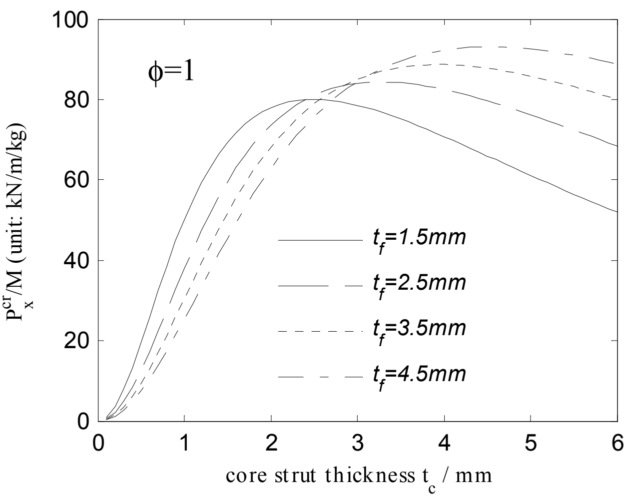

Figure 11: Influence of core strut thickness t_c (h_c = 0.03m, d = 0.0424m)

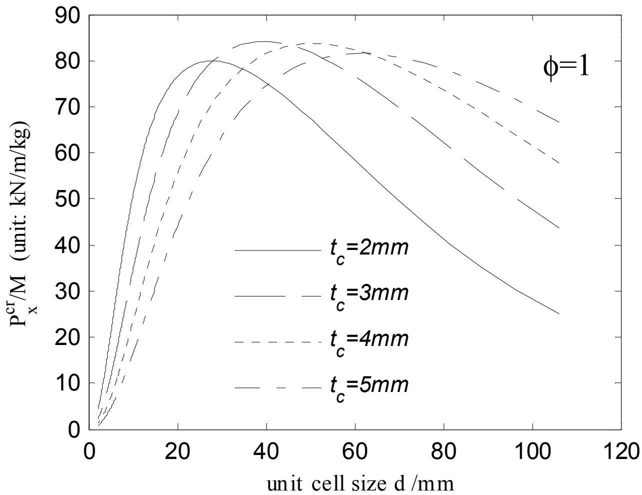

Figure 12: Influence of unit cell size d (h_c = 0.03m, t_f = 0.0025m)

weight M. The ratio of P_x^{cr}/M is introduced to denote the buckling load per unit weight.

Fig. 11 shows the influence of core strut thickness. At each curve the ordinate value climbs up to the peak and then falls. The peak values increase as t_f grows. Fig. 12 shows the influence of unit cell size d. As d grows, the ordinate value climbs to the top and then drops. The peak values of each curve first increase as t_c grow from 2mm to 3mm, then decrease as t_c grow to 4mm. It's obvious that optimal values of d and t_c can be obtained by picking out the largest peak value of P_x^{cr}/M. It's easy to be accomplished by a small computer program. In this example the optimal values of d and t_c are 42.43mm (25 unit cells in both directions) and 3.28mm, respectively.

5 Conclusions

The present study deals with the vibration and buckling of truss core sandwich plates on an elastic foundation subjected to in-plane compressive loads. Natural frequencies are obtained using first order shear deformation theory after a homogenization procedure. In general the applied compressive loads reduce the natural frequencies while tensile loads raise them. The effect of foundation stiffness on buckling loads and modes is discussed. It's found that the foundation stiffness has a most significant influence on the first mode and the intersection point P changes as K varies. In the end, the geometric parameters of a sandwich plate are optimized to obtain strongest buckling resistance per unit weight. The homogenization procedure brings about great savings in computational effort. The accuracy of the solutions is proved by the 3D FE results.

Acknowledgement: The authors are grateful for the support by National Natural Science Foundation of China under grant No. 90916007.

References

Deshpande, V. S.; Ashby, M. F.; Fleck, N. A. (2001): Foam topology bending versus stretching dominated architectures. *Acta Materialia*, vol. 49, no. 6, pp. 1035-1040.

Deshpande, V. S.; Fleck, N. A. (2001): Collapse of truss core sandwich beams in 3-point bending. *Int J Solids Struct*, vol. 38, no. 36-37, pp. 6275-6305.

Hutchinson, J.W.; Xue, Z. Y. (2004): A comparative study of impulse-resistant metal sandwich plates. *Int J Impact Eng*, vol. 30, no. 10, pp. 1283-1305.

Johnson, A. F.; Sims G. D. (1986): Mechanical-Properties and design of Sandwich Materials. *COMPOSITES*, vol. 17, no. 4, pp. 321-328.

Khoshravan, M. R.; Hosseinzadeh, M.(2009): Optimization of a Sandwich Structure Using a Genetic Algorithm. *CMES: Computer Modeling in Engineering & Sciences*, vol. 45, no. 2, pp. 179-206.

Liu, T.; Deng, Z.C.; Lu, T.J. (2007): Structural modeling of sandwich structures with lightweight cellular cores. *Acta Mech Sinca*, vol.23, no. 5, pp. 545-559.

Lok, T. S.; Cheng, Q. H. (2000): Elastic stiffness properties and behavior of truss-core sandwich panel. *J Struct Eng-ASCE*, vol.126, no. 5, pp. 552-559.

Lok, T. S.; Cheng, Q. H. (2000): Free vibration of clamped orthotropic sandwich panel. *J Sound Vib*, vol. 229, no. 2, pp. 311-327.

Lu, T. J.; Valdevit, L.; Evans, A. G. (2005): Active cooling by metallic sandwich structures with periodic cores. *Prog. Mater. Sci*, vol. 50, no. 7, pp. 789-815.

Mindlin, R. D. (1951): Influence of rotatory inertia and shear on flexural motions of isotropic, elastic plates. *J Appl Mech*, vol. 18, pp. 31-38.

Pahr, D. H.; Rammerstorfer, F. G. (2006): Buckling of honeycomb sandwiches: Periodic finite element considerations. *CMES: Computer Modeling in Engineering & Sciences*, vol. 12, no. 3, pp. 229-241.

Qiu, X.; Deshpande, V. S.; Fleck, N. A. (2003): Finite element analysis of the dynamic response of clamped sandwich beams subject to shock loading. *EUROPEAN JOURNAL OF MECHANICS A-SOLIDS*, vol. 22, no. 6, pp. 801-814.

Rabczuk, T.; Kim, J.Y.; Samaniego, E.; et al. (2004): Homogenization of sandwich structures. *Int J Numer Methods Eng*, vol. 61, no. 7, pp. 1009-1027.

Tapp, C.; Hansel, W.; Mittelstedt, C.; et al. (2004): Weight-minimization of sandwich structures by a heuristic topology optimization algorithm. *CMES: Computer Modeling in Engineering & Sciences*, vol. 5, no. 6, pp. 563-573.

Vinson, J. R. (1999): *The Behavior of Sandwich Structures of Isotropic and Composite Materials*. Technomic Publishing Company.

Wallach, J. C.; Gibson, L. J. (2001): Mechanical behavior of a three-dimensional truss material. *Int J Solids Struct*, vol. 38, no. 40-41, pp. 7181-7196.

Wicks, N.; Hutchinson, J. W. (2001): Optimal truss plates. *Int J Solids Struct*, vol. 38, no. 30-31, pp. 5165-5183.

Xue, Z.Y.; Vaziri, A.; Hutchinson, J.W. (2005): Non-uniform hardening constitutive model for compressible orthotropic materials with application to sandwich plate cores. *CMES: Computer Modeling in Engineering & Sciences*, vol. 10, no. 1, pp. 79-95.

Yungwirth, C. J.; Wadley, H. N. G.; O'Connor, J. H.; et al. (2008): Impact response of sandwich plates with a pyramidal lattice core. *Int J Impact Eng*, vol. 35, no. 8, pp. 920-936.

Ziegler, E.; Accorsi, M.; Bennett, M. (2004): Continuum plate model for lattice block material. *Mech Mater*, vol. 36, no. 8, pp. 753-766.